NASA Technical Memorandum 83735

Improved Methods of Vibration Analysis of Pretwisted, Airfoil Blades

K. B. Subrahmanyam and K. R. V. Kaza
Lewis Research Center
Cleveland, Ohio

Prepared for the
XVIth International Congress of Theoretical and Applied Mechanics
cosponsored by the International Union of Theoretical and Applied
Mechanics (IUTAM) and the Technical University of Denmark
Lyngby, Denmark, August 19–25, 1984

NASA

IMPROVED METHODS OF VIBRATION ANALYSIS OF PRETWISTED, AIRFOIL BLADES

K. B. Subrahmanyam* and K. R. V. Kaza**
National Aeronautics and Space Administration
Lewis Research Center
Cleveland, Ohio 44135

SUMMARY

Vibration analysis of pretwisted blades of asymmetric airfoil cross section is performed by using two mixed variational approaches, one proposed by Dean and Plass, and the other by Reissner. Numerical results obtained from these two methods are compared to those obtained from an improved finite-difference method developed by the authors, and also to those given by the ordinary finite-difference method. The relative merits, convergence properties and accuracies of all four methods are studied and discussed. The effects of asymmetry and pretwist on natural frequencies and mode shapes are investigated. The improved finite-difference method is shown to be far superior to the conventional finite-difference method in several respects. Close lower bound solutions are provided by the improved finite-difference method for untwisted blades with a relatively coarse mesh while the mixed methods have not indicated any specific bound.

INTRODUCTION

Turbine and compressor blades, helicopter rotor blades and propeller blades are generally pretwisted and possess asymmetric airfoil cross sections. For such blades, the centroid, center of flexure and center of torsion are noncoincident. General displacements of an asymmetric blade, even without pretwist, consist of translations coupled with rotations. Duncan, Ellis and Scruton (ref. 1) showed that for long members having rigid or quasi-rigid support, the center of flexure and torsion center are very nearly coincident. Carnegie (ref. 2) extended their work for asymmetric airfoil blades and determined the coordinates of the center of flexure with respect to the centroid of the blade cross section. When a blade of asymmetric airfoil cross section vibrates, coupled bending-torsion vibrations occur. Coupling between the bending motions in the two principal directions will be intensified due to pretwist of the blade. Further, an increase in torsional rigidity, over and above that due to St. Venant, takes place due to pretwist. For blades having low aspect ratios and a wide range of thickness ratios, the effect of warping rigidity is very important (ref. 3).

The foundations of the coupled flexure-torsion theories are based on the thin-walled open section formulation and date back to 1936 when Wagner (ref. 4) derived the relation between twisting moment and torsional rotation for the case of nonuniform torsion. The coupled bending-torsion equations of motion were derived by Garland (ref. 5), Gere and Lin (ref. 6), Houbolt and

*NBKR Institute of Science and Technology, Mechanical Engineering Department, Vidyanagar 524 413, India and NRC-NASA Research Associate.
**Research Scientist.

Brooks (ref. 7), Montoya (ref. 8) and Yu (ref. 9), among others, using the classical Euler-Bernoulli theory allowing for various complexities. Using the Timoshenko beam theory, which allows for shear deflection and rotary inertia effects, and incorporating further complexities, the coupled equations of motion were derived by Carnegie (ref. 10), Rao and Rao (ref. 11) and Subrahmanyam, Kulkarni and Rao (ref. 12) among others. Recent research in helicopter and turbo-prop blades indicates that the linear equations of motion are inadequate for establishing flutter boundaries. Geometric nonlinear theory is to be used with various degrees of complexity. Some such theories were presented by Hodges and Dowell (ref. 13), Rosen and Friedmann (ref. 14), and Kaza and Kvaternik (ref. 15) among others.

Several methods of solution of vibration problems are available. Broadly, these are classified as belonging to either the continuum model approach or to the discrete model approach. A comprehensive review of the work done using the various methods in blade vibration area can be found in the review articles by Rao (ref. 16) and Leissa (ref. 17) among others.

An examination of the published literature reveals that among the various methods used for solution of the differential equations of motion, the first-order finite-difference method has attracted the greatest attention while relatively few works exist which use higher-order finite-differences. Even in those few works using second-order central differences either the approximations made to eliminate fictitious stations were not good enough to give accuracy superior to first-order theory results (ref. 18) or a method of using forward or backward differences at beam boundaries was used to avoid the fictitious stations (ref. 19). An improvement to the second order finite-difference method was made by the present authors and this refined method was applied to uncoupled vibration analysis of tapered cantilever beams in (ref. 20), and to pretwisted tapered blades executing coupled bending-bending vibrations in (ref. 21). However, the applicability of the method for vibration analysis of pretwisted asymmetric blades has not been investigated.

Another area, currently receiving considerable attention, is the utilization of mixed or hybrid variational techniques for vibration analysis. Among these mixed variational principles, the Reissner method (ref. 22) has received the greatest attention. For solution of the dynamic vibratory problems, the usual way of formulating the dynamic principle is to consider the difference of the kinetic energy and the Reissner functional, consisting of contributions from potential and complementary energies together with the work done by the body forces and surface tractions (ref. 23), and to minimize the same according to the Ritz process. One thus has the flexibility to vary displacements and stresses independently and can obtain simultaneously good distributions of all the independent parameters. Another more flexible way of formulating the dynamic variational functional is demonstrated by Dean and Plass (ref. 24) where the kinetic energy effects were incorporated by using linear momentum density in conjunction with the Reissner functional. This way to include angular momentum and rotary inertia effects was demonstrated by the present first author's earlier work (refs. 25 and 26), and it was observed that both mixed variational principles (refs. 22 to 24) lead to identical results if identical shape functions and beam kinematics were used in the analysis. However, attempts to incorporate coupling between the flexural and torsional degrees of freedom were not made so far. An important advantage offered by the Dean and Plass method is that one can handle the gyroscopic forces in the

vibratory problem in a straightforward manner. Since this variational principle contains products of linear or angular momenta and the corresponding velocities in the kinetic energy equivalent, and since the gyroscopic forces also are functions of velocities, the variational functional possesses consistently first order time derivative functions. Unlike the Reissner or potential energy methods, which require either a transformation procedure or other more complicated methods for solution (refs. 27 and 28), the Dean and Plass method leads directly to a standard eigenvalue problem.

The objectives of the present work are: (1) to apply the first, and second order finite-difference methods, the Dean and Plass method and the Reissner method for the general case of vibration with coupling between bending and torsional degrees of freedom; (2) to assess the computational advantages and disadvantages of each method; and (3) to study the effects of pretwist and asymmetry in coupling the component modes. Numerical results from all four methods will be presented and comparisons will be made to those from other existing theoretical and experimental results (refs. 29 to 33).

SYMBOLS

A	area at any section
$\underset{\sim}{A},\underset{\sim}{B},\underset{\sim}{C},\underset{\sim}{D}$	matrices
$A_i,B_i,\ldots I_i$	arbitrary parameter in shape functions
$\bar{B}_i$	body force distribution
C	torsional stiffness
C_1	warping rigidity
c.f.	center-of-flexure of blade cross section
E	Young's modulus
f_i,g_i,h_i	shape functions
G	modulus of rigidity
h	length of each elemental beam segment
I_{x1x1}	second moment of area of a cross section about x_1x_1 axis
I_{y1y1}	second moment of area of a cross section about y_1y_1 axis
I_{x1y1}	product of inertia of a cross section about x_1x_1 and y_1y_1 axes
I_{xx}	second principal moment of area of cross section about xx- direction at root section
I_{yy}	second principal moment of area of cross section about yy- direction at root section
I_{cf}	polar moment of inertia about c.f., $I_{x1x1} + I_{y1y1} + A(r_x^2+r_y^2)$

I_D	Dean and Plass dynamic variational functional
I_R	dynamic Reissner functional
$\bar{I}_D, \bar{I}_R$	time averaged values of I_D and I_R respectively
i,j	dummy indices
k	number of terms in the assumed solutions
L	length of blade
M_x, M_y	bending moments
n	number of beam segments
P_n	natural radian frequency
r_x, r_y	coordinates of center-of-flexure with respect to centroid at any section distant η from root
$\bar{r}_x, \bar{r}_y$ etc.	r_x/L, r_y/L etc.
r_{xo}, r_{yo}	coordinates of center of flexure with respect to centroid at the root section
r_{cf}	polar radius of gyration, $\sqrt{\{(I_{x1x1} + I_{y1y1})/A + r_x^2 + r_y^2\}}$
S1	part of boundary over which surface fractions are prescribed
$\bar{T}_i^{(\tau)}$	surface fractions
t	time
T	kinetic energy
T_θ	twisting moment
U_i	displacement field
U_x, U_y, U_z	displacement in x, y, and z directions
ν	volume
P_i	components of linear momentum per unit volume
P_{x1}, P_{y1}	linear momentum density along x_1x_1 and y_1y_1 directions, respectively
P_θ	angular momentum density
x,y	displacement of center-of-flexure in xx, yy directions respectively
x_1, y_1	displacements of centroid in x_1x_1, y_1y_1 directions respectively
$\dot{x}, \dot{y}; \dot{x}_1, \dot{y}_1$	coordinates measured with respect to center of flexure and centroid respectively

$x_1x_1, y_1y_1; xx, yy$	coordinates axes through centroid and center of flexure respectively
zz	longitudinal axis
z	coordinate distance measured along the length of blade from root section
ϵ_{ij}	strains
θ	torsional deflection
ρ	mass density
τ_{ij}	stresses
ϕ_c	warping function
γ	pretwist angle
η	axial fractional length z/L
$(\ )'$	prime denotes differentiation with respect to z
$(\dot{})$	dot over a parameter represents differentiation with respect to time, t
$(\dot{})'$	successive differentiation with respect to z and t
$\phi_{c,x1}$; $U_{i,j}$ etc.	$\frac{\partial \phi_c}{\partial x_1}$, $\frac{\partial U_i}{\partial x_j}$ etc.
$\bar{x}, \bar{y}, \bar{\theta}$	relative amplitudes

DEVELOPMENT OF FREQUENCY EQUATIONS

Frequency Equations by Finite-Difference Methods

For a pretwisted blade of asymmetric airfoil cross section having a total pretwist angle γ over length L, the equations of motion (A18), appendix A, assume the following nondimensional form:

$$a_1 \frac{d^4y}{d\eta^4} + b_1 \frac{d^3y}{d\eta^3} + c_1 \frac{d^2y}{d\eta^2} + d_1 \frac{d^4x}{d\eta^4} + e_1 \frac{d^3x}{d\eta^3} + f_1 \frac{d^2x}{d\eta^2} = g_1 p_n^2 y + h_1 p_n^2 \theta \qquad (1)$$

$$a_2 \frac{d^4y}{d\eta^4} + b_2 \frac{d^3y}{d\eta^3} + c_2 \frac{d^2y}{d\eta^2} + d_2 \frac{d^4x}{d\eta^4} + e_2 \frac{d^3x}{d\eta^3} + f_2 \frac{d^2x}{d\eta^2} = g_2 p_n^2 x + h_2 p_n^2 \theta \qquad (2)$$

$$a_3 \frac{d^2\theta}{d\eta^2} = b_3 p_n^2 y + c_3 p_n^2 x + d_3 p_n^2 \theta \qquad (3)$$

The coefficient a_1, b_1 ... h_1, a_2, b_2 ... h_2, a_3 ... d_3 are all functions of η and are presented in appendix B.

In implementing a finite difference procedure for the solution of the equations of motion, one substitutes the finite-difference expressions for the derivatives in the differential equations and eliminates the fictitious stations out side the beam domain by enforcing the boundary conditions. The resulting equations contain the displacements x_i, y_i and θ_i at an arbitrary station i. The coupled equations are then evaluated at each station of the beam divided into n segments, i = 1,2...n. One thus obtains a set of 3n simultaneous equations.

In references 20 and 21, the present authors developed a refined procedure for eliminating fictitious stations that arise in using second order central differences. Use is made of the recursive relations and the finite-difference expressions reported in reference 20 in the present investigation, and the resulting equations are represented in the familiar form of the eigenvalue problem

$$\begin{bmatrix} \underline{A} & \underline{B} & \underline{Q} \\ \underline{C} & \underline{D} & \underline{Q} \\ \underline{Q} & \underline{Q} & \underline{E} \end{bmatrix} \begin{Bmatrix} \{x_i\} \\ \{y_i\} \\ \{\theta_i\} \end{Bmatrix} = P_n^2 \begin{bmatrix} \underline{Q} & \underline{F} & \underline{G} \\ \underline{H} & \underline{Q} & \underline{I} \\ \underline{J} & \underline{K} & \underline{L} \end{bmatrix} \begin{Bmatrix} \{x_i\} \\ \{y_i\} \\ \{\theta_i\} \end{Bmatrix} \qquad (4)$$

In the preceding equation, $\underline{A}$, $\underline{B}$, $\underline{C}$, $\underline{D}$ and $\underline{E}$ are all square matrices of order (nxn), $\{x_i\}$, $\{y_i\}$ and $\{\theta_i\}$ are column matrices containing the linear and torsional displacements of the n-stations and $\underline{F}$, $\underline{G}$, $\underline{H}$, $\underline{I}$, $\underline{J}$, $\underline{K}$ and $\underline{L}$ are diagonal. The matrix $\underline{Q}$ is a null matrix. Further, each submatrix $\underline{A}$, $\underline{B}$, $\underline{C}$ or $\underline{D}$ has a band width of five for the first-order theory and seven for second-order theory. The submatrix $\underline{E}$ has a band width of three for first-order theory and five for second-order theory. The matrices $\underline{A}$, $\underline{B}$, $\underline{C}$, $\underline{D}$ and $\underline{E}$ are nonsymmetric in first and second order finite-difference applications. For brevity elements of these matrices are not presented, but one can easily develop these matrices with the help of references 20 and 21.

Frequency Equation from the Dean and Plass Principle

The Dean and Plass dynamic variational functional is developed in appendix A and has the functional relationship of the form

$$I_D = I_D\,(x,y,\theta,P_{x1},P_{y1},P_\theta,M_x,M_y,T_\theta,n,t) \qquad (5)$$

The parameters in the functional given by equation (5) are independent of each other and depend only on n and t.

The following shape functions in series form (refs. 23 and 25) are assumed for solution of the coupled bending-bending-torsion vibration problem:

$$x = \sum_{i=1}^{k} A_i\,(R_1\,n - R_2\,n^2 + R_3\,n^3)\,n^i \qquad G(t) = \sum_{i=1}^{k} A_i\,f_i(n)\,G(t)$$

$$P_{x1} = \sum_{i=1}^{k} B_i\,f_i\,(n)\,H(t)$$

$$y = \sum_{i=1}^{k} C_i f_i(\eta)\, G(t)$$

$$P_{y1} = \sum_{i=1}^{k} D_i f_i(\eta)\, H(t)$$

$$M_x = \sum_{i=1}^{k} E_i R_4 (1-\eta)^i G(t) = \sum_{i=1}^{k} E_i g_i(\eta)\, G(t)$$

$$M_y = \sum_{i=1}^{k} F_i g_i(\eta)\, G(t)$$

$$\theta = \sum_{i=1}^{k} G_i \eta^i (1-R_5 \eta) \quad G(t) = \sum_{i=1}^{k} G_i h_i(\eta)\, G(t)$$

$$T_\theta = \sum_{i=1}^{k} H_i g_i(\eta)\, G(t)$$

$$P_\theta = \sum_{i=1}^{k} I_i h_i(\eta)\, H(t) \tag{6}$$

The parameters $R_1, R_2 \ldots R_5$, $G(t)$, $H(t)$ etc. are defined in appendix B. The shape functions given in equation (2) satisfy the boundary conditions (ref. 12) applicable to a cantilever beam fixed at $\eta = 0$ and free at $\eta = 1$. Substituting equations (6) and their appropriate derivatives into equation (A13), eliminating the time dependence according to the averaging procedure

$$\bar{I}_D = \int_0^{2\pi/P_n} I_D dt \tag{7}$$

and applying the Ritz process to minimize $\bar{I}_D$ with respect to the arbitrary parameters, that is,

$$\frac{\partial \bar{I}_D}{\partial A_k} = \frac{\partial \bar{I}_D}{\partial B_k} = \ldots \frac{\partial \bar{I}_D}{\partial I_k} = 0, \; k = 1,2, \ldots K, \tag{8}$$

one obtains the frequency equation which can be written as

$$\underline{A} + P_n \underline{B} = 0 \tag{9}$$

In equation (9), $\underline{A}$ and $\underline{B}$ are symmetric square matrices. For brevity elements of these matrices are not presented here.

Frequency Equation from the Reissner Method

The Reissner variational functional (ref. 22) is given by

$$I_R = \iiint_V \left[\frac{\rho \dot{u}_i \dot{u}_i}{2} - \{\tau_{ij}\, \varepsilon_{ij} - U_o^*(\tau_{ij})\} + \bar{B}_i\, U_i \right] dv - \iint_{s1} \bar{T}_i^{(\gamma)} u_i\, ds \qquad (10)$$

Neglecting body forces, surface tractions, shear deflection, rotary inertia, thermal and rotational effects, one can show that (ref. 12)

$$I_R = \int_0^{2\pi/P_n} \int_0^L \left[\frac{\rho A}{2} (\dot{y} + r_x \dot{\theta})^2 + \frac{\rho A}{2} (\dot{x} + r_y \dot{\theta})^2 + \frac{\rho I_p}{2} \dot{\theta}^2 \right.$$

$$\left. + M_x y'' + M_y x'' - T_\theta \theta' + \frac{T_\theta^2}{2C} + \frac{M_x^2 I_{y1y1} - 2M_x M_y I_{x1y1} + M_y^2 I_{x1x1}}{2E\,(I_{x1x1} I_{y1y1} - I_{x1y1}^2)} \right] dz\, dt \qquad (11)$$

Using similar shape functions as were used for the Dean and Plass method and proceeding on the same lines as described earlier, one can obtain the frequency equation which can be written as

$$\underset{\sim}{C} + P_n^2 \underset{\sim}{D} = 0 \qquad (12)$$

Matrices $\underset{\sim}{C}$ and $\underset{\sim}{D}$ are symmetric, the elements of which are not presented here to save space.

METHOD OF SOLUTION

The eigenvalue problems given by equations (4), (9) and (12) were solved by using a standard eigenvalue extraction routine. This library routine determines all the eigenvalues and the associated eigenvectors. For the eigenvalue problem formulation using mixed variational approaches, certain integrations were to be performed numerically. This was accomplished by using a 15 point Gaussian quadrature formula. The computer programs developed in FORTRAN language were run on an IBM 370 computer at the NASA Lewis Research Center. The lowest ten coupled frequencies and associated mode shapes were determined for studying the effects of asymmetry and pretwist in coupling the modes using typical airfoil blade data (ref. 2). Results are presented and discussed in what follows.

RESULTS AND DISCUSSION

In order to study the accuracies and computational efficiencies of the four methods discussed in this report, airfoil blade data developed by Carnegie (ref. 2) and used by Carnegie and others for numerical calculations (refs. 29 to 32), was adopted. Such numerical data pertaining to the typical blade profile shown in figure 1 is presented in tables I and II. It may be noted that

the coordinates of the center-of-flexure measured with respect to the centroid assumed in this report are the experimental values (ref. 2). Further, the values of torsional rigidity used in the present calculations are taken from the experimental data presented by Carnegie (ref. 29). By using the numerical data presented in tables I and II, results obtained from the four methods are compared mutually and to those existing in the literature in what follows.

Relative Convergence Rates and Accuracies

A typical set of results obtained by using first and second-order central difference formulations and with various mesh sizes are presented in table III. Results given by both first and second order theories are lower bounds for an untwisted blade. No specific bound is given by the finite-difference methods for twisted blade cases (ref. 21).

From the results presented in table III, one can state that the convergence shown by the second order theory is much more rapid than the first. Further, the accuracy of the converged results can be assessed by comparing the natural frequencies given by the finite-difference solution with a given mesh size (number of beam segments) to corresponding extrapolated results using the Richardson extrapolation procedure (ref. 34). For this purpose, the results using $n = 10$, 20 and 30 in the second order theory are extrapolated and are presented in the last column of table III. In comparison with the extrapolated result, the first-order theory with $n = 60$ shows maximum errors of the magnitudes of about 0.4 percent and 0.64 percent in the lowest seven coupled mode frequencies for the cases $\gamma = 0^\circ$ (untwisted blade) and $\gamma = -30^\circ$ (clockwise pretwisted blade) respectively. Corresponding maximum errors from the second order theory are 0.075 percent and 0.322 percent when the beam is divided into 30 segments ($n = 30$).

From these observations, it is concluded that the second-order theory produces results with accuracies of practical interest with a coarse mesh size. Results given by the second order theory with $n = 30$ are superior to those from the conventional first order theory with $n = 60$ and thus, the extrapolation procedure is not necessary when the improved second order theory is used with a suitable mesh size.

In order to assess the relative merits of the two mixed variational principles namely the Reissner method and the Dean and Plass method, identical shape functions were assumed for the independent variables in both methods. Natural frequencies were determined for the two typical values of pretwist ($\gamma = 0^\circ$ and $\gamma = -30^\circ$) considered earlier while using finite-difference approaches. Natural frequencies were obtained by varying the number of terms in the assumed solution for each shape function. The convergence shown by the methods was found to be almost identical. These results are shown in tables IV(a) and (b). This is an expected trend since the momentum functions were chosen to have identical shape functions as those corresponding to the respective displacement functions, thus, making the two variational methods numerically equivalent. However, the flexibility of independent variations of displacements and momenta can effectively be utilized by incorporating different forms of shape functions as shown in reference 24 and 26, consistent with the boundary conditions.

From the identical convergence pattern produced by both mixed variational principles, the accuracy of the theoretical development of the Dean and Plass functional is conclusively verified. A further comparison of the results presented in table IV to the corresponding sets presented in table III indicates that the lowest seven coupled modes obtained by using a six-term solution of the Dean and Plass or Reissner method agree very closely with the extrapolated results from finite-difference solutions. Furthermore, the mixed variational principles considered here have not shown any specific bound, and the results presented in table IV can be seen to have an oscillatory nature.

Finally, a comparison of the present converged results is made to the theoretical and experimental results available in the literature. Such a comparison is shown in figure 2. Both clockwise and anticlockwise pretwists ranging from 0° to 89° were considered. Results produced by finite-difference procedure using second-order central differences with $n = 30$ and those produced by the Reissner and, Dean and Plass methods with $K = 6$ were close for the lowest seven modes. These results agree very closely with the theoretical results of Carnegie et al. (ref. 30) obtained by using a transformation technique and also with experimental results. Although not shown here, the mode shapes obtained by using the various methods were also close.

Effects of Pretwist and Asymmetry in Coupling the Modes

For blades of doubly symmetric cross section, the effect of pretwist in coupling the two principal bending motions has been well understood in the published literature. Rosard (ref. 35) observed the effect of pretwist on the coupled bending-bending frequencies for the first time. Later, Carnegie et al. (refs. 29 to 31), Rao (ref. 16) and the present authors (refs. 3, 21, and 23), among others, studied the effect of pretwist on the natural frequencies and mode shapes. However, the combined effects of asymmetry and pretwist on the natural frequencies and mode shapes have not been completely understood.

In order to understand any specific coupling trends that may exist in the coupled bending-bending-torsional frequencies of pretwisted blades of asymmetric airfoil cross section, it is necessary to establish the coupling trends for simple cases of blade geometry first. For this purpose, using the second order finite-difference method with 30 beam segments, the uncoupled bending and torsional frequencies and mode shapes were determined by assuming $r_{xo} = 0$, $r_{yo} = 0$ and $\gamma = 0$ in the general computer program. These natural frequencies are presented in table V under column 2. In this table, the frequencies of the beam vibration in the flexible plane are designated by F1, F2, ..., F5 for the lowest five modes, those in the stiffer plane are designated by S1, S2 for the lowest two modes while T1, T2 and T3 represent the lowest three torsional frequencies in the increasing order. The coupled bending-bending frequencies and the associated mode shapes were next determined by successively assigning different pretwist angles. The coupled bending-bending frequencies for typical pretwist angles are presented in table V under columns 3 to 6. Although the mode shapes were determined for all the pretwists considered here, only one such set (pretwist angle of 89°) is presented in figure. 3. Using these uncoupled mode shapes or the coupled bending-bending mode shapes, one can classify any coupled bending-torsion or coupled bending-bending-torsion mode shape as belonging closely to a basic mode category. Further results were generated for various combinations of the coordinates of asymmetry and

pretwist angles. The modes were then classified as belonging to a basic mode category by examining the associated mode shapes in relation to either the uncoupled mode shapes or to the coupled bending-bending mode shapes. These results are tabulated in tables VI to VIII. Thus, in table VI, for blades with r_{xo} = 0.193 mm, r_{yo} = 0 are presented, in table VII those for r_{xo} = 0, r_{yo} = 1.1938 mm are shown while in table VIII, the results of general asymmetric airfoil blade with r_{xo} = 0.193 mm, r_{yo} = 1.1938 mm are listed for various angles for pretwist. It may be noted that the frequencies are not necessarily in an increasing order as the mode number is increased since the modes are classified as belonging to a basic mode category. Only one set of coupled bending-bending-torsion mode shapes are presented in figure 4 for the case $\gamma = 89^\circ$ for brevity. The general coupling trends as observed from these results are presented below.

(1) For pretwisted blades of doubly symmetric cross section, strong coupling exists between the second uncoupled flapwise mode (F2) and fundamental uncoupled chordwise mode (S1). As pretwist increases, the lower frequency decreases and the higher frequency increases to form the corresponding coupled frequencies. Similar coupling between the uncoupled modes S2 and F5 exists but the magnitude of frequency variations are more severe for the set (F2, S1) than for the set (S2, F5). This frequency variation trend is consistent with earlier observations reported in references 23 and 35. The coupled bending-bending mode shapes obtained in the present investigation are compared to those in reference 33. Consistent trends have been observed in all the results compared.

(2) For untwisted blades with asymmetry about only one plane, coupling between bending in one principal direction and torsion occurs. Results for such a case with r_{yo} = 0 are shown in column 3 of table VI, and for the case r_{xo} = 0 in table VII. From the results presented in table VI, one can observe that the frequencies corresponding to (F2, T1) and (F3, T2) couple in such a way that the lower uncoupled frequency in each pair is reduced and the higher one is increased to form the corresponding coupled bending-torsion frequencies. Although not shown here, similar coupling trends exist for the pairs (F4, T3) and (F5, T4). Similar coupling trends are observed for the coupled modes having coupling between chordwise bending and torsional motions. This coupling trend is shown by the frequency pair (S1, T1) in table VII. Although not shown, the frequency pair (T3, S2) also shows similar coupling trends.

(3) For pretwisted blades with asymmetry about only one plane, the coupling trends are combinations of those discussed in (1) and (2) above. A careful examination of the results presented in tables VI and VII for various values of pretwist angles in relation to the corresponding ones in table V indicates that a specific trend in the three close frequency values corresponding to F2, S1 and T1 modes exists. The frequencies corresponding to the pretwisted symmetric blade listed in table V will be further coupled because of asymmetry in such a way that the lower two frequencies will be reduced and the highest one will be increased to result in the coupled bending-bending-torsion frequencies. Other secondary coupling trends are observed for the frequency pair (T2, F4) when the frequencies are very close to one another, in table VII, and for all pretwist angles in table VI. The reason for this is that the flap-torsion coupling is more important for blades having a symmetry about the chord (table VI) than for those with asymmetry about the chord (table VII).

Similar coupling trends exist for the frequencies corresponding to the frequency triplet (T3, S2, F5). However, results for these modes are not presented here because obtaining accuracy in these higher mode frequencies would have required a greater number of beam segments.

(4) The coupling trends for pretwisted asymmetric airfoil blades presented in table VIII are similar to those observed for the simpler cases considered earlier. It has been observed that the coordinate r_{yo} is more important than r_{xo} in coupling the component modes.

(5) From the mode shapes obtained for all the cases studied in this investigation, it is observed that the coupled modes which are well separated from a basic torsional mode frequency are not seriously effected by the torsional coupling (refer figs. 3 and 4). These mode shapes can be closely approximated by the corresponding coupled bending-bending mode shapes. For modes which are closer to a basic torsional mode, the extent of torsional coupling must be determined.

The trailing edge deflections calculated in this investigation show close agreement with those presented by Carnegie et al. (ref. 30). Although the trailing edge deflections were determined for all cases of pretwist angles studied, they are not presented in this report for brevity.

Finally, the coupled frequencies were determined for different sets of asymmetry coordinates, (r_{xo} = 2.54 mm, r_{yo} = 1.1938 mm; and r_{xo} = 0.193 mm, r_{yo} = 2.54 mm), to examine whether there are any changes in the coupling trends with large variations in these coordinates. Although these results are not presented here, it was observed that the general coupling trends remain unchanged.

RELATIVE COMPUTATIONAL EFFICIENCIES

In order to evaluate the relative computational efficiencies, the CPU time required by each method for a typical blade example was determined. These values are presented in table IX.

Comparing the CPU times required by firstand second-order finite-difference methods for a given number of beam segments, one can state that both methods require nearly the same amount of CPU time. The maximum variation of CPU time between the two methods is of the order of ± 3 percent. If one considers the level of accuracy for estimation of computational efficiency, the first-order finite-difference method requires a solution with 60 beam segments to match the accuracy of results produced by the second-order finite-difference method with n = 30. The computation time required for first-order theory would be nearly 13 times that required by the present improved second order theory. Finally, if one considers an extrapolation procedure as a suitable alternative, then, both first and second order theories presented here are capable of taking the advantage. Thus, it is preferable to use the present improved finite-difference procedure as compared to the classical first-order theory.

When a comparison is made between the computational times required by the Reissner and the Dean and Plass methods, one observes that the Dean and Plass method requires nearly twice as much time as the Reissner method. For the

particular example considered here with identical shape functions in both methods, it has been observed that the convergence trends and accuracies given by these two methods are identical. Thus, for the class of vibratory problems treated here, it is advantageous to use the Reissner mixed variational principles as compared to the Dean and Plass principle. On the other hand, for solution of problems having gyroscopic forces (Coriolis accelerations), the usual formulation by the potential energy method or the Reissner method requires a transformation of the time dependent variables by a linear transformation to attain the eigenvalue problem in a standard form (ref. 28) while the Dean and Plass method seems to offer a more direct solution facility. This advantage together with any associated computational advantages relative to the existing approaches are yet to be assessed.

When a choice is to be made between the finite-difference procedures and the energy methods for potential computational needs, it appears that energy methods have a great deal to offer when computational time is the principle constraint. As can be seen from tables III and IV, one can obtain the lowest seven coupled modes accurately with a six-term solution using the Reissner method. These results can be obtained in about 13 percent of the CPU time required by the second order finite-difference method. While making this comparison, it may be noted that the symmetry of the matrices given by the mixed variational principles is not effectively utilized in the solution procedure using the IMSL routine EIGZF (ref. 36). If the symmetric nature of these matrices were effectively used, the computation time might be further reduced. Similarly, no advantage has been taken of the banded nature of the matrices in using the finite-difference methods. If this advantage were utilized in the computational scheme, some CPU time and considerable memory size might be saved.

Finally, the mathematical implications of the various analytical methods are considered.

In the two finite-difference procedures presented, the formulation of the eigenvalue problem does not require great mathematical skills or judgment. Anyone with a reasonable mathematical background can formulate and solve the problem, once the recursive relations for elimination of the fictitious stations are provided. These methods require no integrations and thus the necessity of using any numerical quadrature formulae is avoided. For the class of problems treated so far, no numerical instabilities were observed, meaning that the finite-difference procedures lead to numerically well-posed problems. Further, for untwisted blades, the coupled or uncoupled frequencies converge from below and close lower bound solutions are obtained.

Considering the mixed variational principles, one starts with a mathematically stationary functional (which possesses neither a maximum nor a minimum) rather than a minimum energy concept. Consequently, the natural frequencies do not specify any bound but oscillate closely around a converged exact value. The convergence rates and accuracies depend largely on the choice of shape functions. The final equations require evaluation of definite integrals using a numerical quadrature formula generally. Thus, some judgment and skill of the investigator are needed when the mixed variational principles are used. Furthermore, the matrices are usually ill-conditioned, and some form of scaling is necessary if one wishes to evaluate the frequencies by determinant search. While the mass and stiffness matrices are symmetric, they are not necessarily

nonsingular. One may thus have computational problems if inversions are needed. These problems could however be obviated by condensation or by rewriting the equations so that the elements along the leading diagonal are nonzero, thus losing the symmetry condition. Once the mixed variational principle is formulated and suitable shape functions are assumed, the solution procedure is rather straightforward however.

In conclusion, each class of methods has certain distinct advantages and one can choose a method depending on the constraints at hand, considering the advantages and disadvantages. All the methods presented have capabilities of producing accuracies of practical interest. The second order finite-difference procedure is definitely superior to the classical approach while for the class of problems considered here, the Reissner method is superior to the Dean and Plass principle.

CONCLUDING REMARKS

The coupled bending-bending-torsion vibrations of pretwisted blades of asymmetric airfoil cross section are analyzed by solving the governing coupled equations of motion using first and second-order finite-difference methods. Alternative approaches of solving the coupled vibration problem are demonstrated by employing two mixed variational approaches, one proposed by Dean and Plass and the other by Reissner. The relative merits, convergence properties and accuracies of all the four methods are discussed. The effects of asymmetry and pretwist in coupling the component modes are studied. In the course of this study, the following conclusions have emerged:

(1) The improved second order finite-difference procedure is far superior to the classical first order procedure. One can use the present improved theory for attaining better accuracies while using smaller computation time and effort than that required by ordinary finite-difference procedure.

(2) For untwisted blades performing coupled bending-bending-torsion vibrations, close lower bound solutions can be obtained by using improved finite-difference procedure. However pretwist disturbs the bound offered by finite-difference procedures. The mixed variational approaches do not indicate any specific bound.

(3) When identical shape functions and beam kinematics are used, the Dean and Plass and the Reissner methods give identical results. However, the Dean and Plass method requires more computational time.

(4) The Dean and Plass method appears to be more advantageous when gyroscopic effects are included in the analysis. Further investigation in this direction appears to be necessary for utilizing the latent potential of this relatively new variational principle.

(5) For general vibratory problems, the variational methods seem to be more appealing in terms of computational space and time. However, some care and judgment of the investigator are required when the mixed variational principles are employed.

The finite-difference method is relatively straight forward and simple. One can apply this approach in a routine manner once the recursive relations are given for elimination of fictitious stations.

(6) The effects of asymmetry and pretwist appear to be difficult to understand at first sight. However, once the coupled frequencies are classified as belonging to a basic mode category as described in this work, the coupling trends can easily be established.

APPENDIX A

DEVELOPMENT OF THE DEAN AND PLASS VARIATIONAL FUNCTIONAL

The Dean and Plass dynamic variational functional (ref. 24) can be written as

$$I_D = \iiint_{\nu} \{(P_i \dot{U}_i - \frac{P_i P_i}{2\rho})\} \, d\nu - I_{RS} \tag{A1}$$

where I_{RS} is the Reissner functional given by (ref. 22)

$$I_{RS} = \iiint_{\nu} \{\tau_{ij}\varepsilon_{ij} - U_o^*(\tau_{ij})\} \, d\nu - \iiint_{\nu} \bar{B}_i U_i d\nu - \iint_{S1} \bar{T}_i^{(\gamma)} U_i ds \tag{A2}$$

Development of the Reissner functional is presented in reference 12 for the general case of asymmetric blade. Only the kinetic energy equivalent of the Dean and Plass dynamic functional will be developed in what follows.

Neglecting the effects of shear deformation, the general displacement field for coupled bending-bending-torsional motion can be written as (ref. 12)

$$U_x = x - y\theta = x_1 - y_1\theta \tag{A2}$$

$$U_y = y + x\theta = y_1 + x_1\theta \tag{A3}$$

$$U_z = -x_1 x_1' - y_1 y_1' + \phi_c \theta' \tag{A4}$$

For the computation of the kinetic energy, one can disregard the effects of longitudinal inertia effects in the total kinetic energy without great loss of accuracy in the final results. It will be assumed that the longitudinal inertia effects are negligible and thus the linear momentum densities about x and y directions take the following forms:

$$P_x = \rho \dot{U}_x = \rho (\dot{x}_1 - y_1\dot{\theta}) \tag{A5}$$

$$P_y = \rho \dot{U}_y = \rho (\dot{y}_1 + x_1\dot{\theta}) \tag{A6}$$

Equations (A5) and (A6) contain terms associated with linear velocities $\dot{x}_1$ and $\dot{y}_1$ together with the angular velocity $\dot{\theta}$. One can explicitly define the linear and angular momenta by defining the linear momenta about $x_1 x_1$, $y_1 y_1$ centroidal directions and angular momentum due to elastic twist independently as follows:

$$P_{x1} = \rho \dot{x}1 \tag{A7}$$

$$P_{y1} = \rho \dot{y}1 \tag{A8}$$

$$P_{\theta} = \left(\frac{\rho I_p \dot{\theta}}{A}\right) \tag{A9}$$

Thus

$$\iiint_{\nu} P_i \dot{U}_i \, d\nu = \int_0^L \int_A \left[(P_{x1} - \rho y_1 \dot{\theta})\ (\dot{x}_1 - y_1 \dot{\theta}) + (P_{y1} + \rho x_1 \dot{\theta})\ (\dot{y}_1 + x_1 \dot{\theta})\right] dA\, dz$$

$$= \int_0^L \left[P_{x1} A \dot{x}_1 + P_{y1} A \dot{y}_1 + P_{\theta} A \dot{\theta}\right] dz \tag{A10}$$

and

$$\iiint_{\nu} \frac{P_i P_i}{2\rho} \, d\nu = \int_0^L \left[\frac{P_{x1}^2 A + P_{y1}^2 A}{2\rho} + \frac{P_{\theta}^2 A^2}{2\rho I_p}\right] dz \tag{A11}$$

The Reissner functional, I_{RS}, can be reduced to the following form for the coupled bending-bending-torsion case neglecting shear deformation, body forces, surface fractions and warping rigidity effects:

$$I_{RS} = - \int_0^L \left[M_x y'' + M_y x'' - T_{\theta} \theta' + \frac{T_{\theta}^2}{2c} + \frac{M_x^2 I_{y1y1} - 2M_x M_y I_{x1y1} + M_y^2 I_{x1x1}}{2E\ (I_{x1x1} I_{y1y1} - I_{x1y1}^2)}\right] dz \tag{A12}$$

Making use of equations (A10) to (A12) in equation (A1), the Dean and Plass dynamic variational functional becomes

$$I_D = \int_0^L \left[P_{x1} A\ (\dot{x} + r_y \dot{\theta}) + P_{y1} A\ (\dot{y} + r_x \dot{\theta}) + P_{\theta} A \dot{\theta} - \frac{P_{x1}^2 A}{2\rho} - \frac{P_{y1}^2 A}{2\rho} - \frac{P_{\theta}^2 A^2}{2\rho I_p}\right.$$

$$\left. + M_x y'' + M_y x'' - T_{\theta} \theta' + \frac{T_{\theta}^2}{2C} + \frac{M_x^2 I_{y1y1} - 2M_x M_y I_{x1y1} + M_y^2 I_{x1x1}}{2\ E\ (I_{x1x1} I_{y1y1} - I_{x1y1}^2)}\right] dz \tag{A13}$$

Treating P_{x1}, P_{y1}, P_{θ}, M_x, M_y, T_{θ}, x, y and θ as independent variables (independent of one another but dependent on z and t) and performing the variational process (ref. 12)

$$\delta^{(1)} I_D = 0 \tag{A14}$$

one obtains the following equations:

$$\left.\begin{aligned}
P_{x1} &= \rho\,(\dot{x} + r_y\dot{\theta}) = \rho\dot{x}_1 \\
P_{y1} &= \rho\,(\dot{y} + r_x\dot{\theta}) = \rho\dot{y}_1 \\
P_{\theta} &= \rho\,(I_{x1x1} + I_{y1y1})\,\dot{\theta}/A = \rho I_p\dot{\theta}/A \\
y'' &= -\frac{(M_x I_{y1y1} - M_y I_{x1y1})}{E\,(I_{x1x1}I_{y1y1} - I_{x1y1}^2)} \\
x'' &= -\frac{(M_y I_{x1x1} - M_x I_{x1y1})}{E\,(I_{x1x1}I_{y1y1} - I_{x1y1}^2)} \\
\theta' &= T_{\theta}/2C
\end{aligned}\right\} \qquad \text{(A15)}$$

$$\left.\begin{aligned}
&-\frac{\partial}{\partial t}(AP_{x1}) + \frac{\partial^2}{\partial z^2}(M_y) = 0 \\
&-\frac{\partial}{\partial t}(AP_{y1}) + \frac{\partial^2}{\partial z^2}(M_x) = 0 \\
&-\frac{\partial}{\partial t}(AP_{x1}r_y + AP_{y1}r_x + AP_{\theta}) + \frac{\partial}{\partial z}(T_{\theta}) = 0
\end{aligned}\right\} \qquad \text{(A16)}$$

$$\left.\begin{aligned}
&\frac{\partial}{\partial z}(M_y) = 0 \text{ at } z = 0, L \text{ or } x \text{ prescribed} \\
&\frac{\partial}{\partial z}(M_x) = 0 \text{ at } z = 0, L \text{ or } y \text{ prescribed} \\
&T_{\theta} = 0 \text{ at } z = 0, L \text{ or } \theta \text{ prescribed}
\end{aligned}\right\} \qquad \text{(A17)}$$

Equations (A15) relate the linear and angular momenta to respective linear or angular velocities, curvatures to bending moments and rate of twist to twisting moment and torsional rigidity. These relations can alternatively be looked upon as stress-strain relations. Equations (A16) represent the conditions of equilibrium or motion. The first two of equations (A16) relate the time rate changes of linear momenta per unit length to corresponding rates of loading (forces per unit length). The last of equations (A16) equates the time rate of change of angular momentum per unit length to the twisting moment (torque) per unit length. Equations (A17) are the boundary conditions associated with the present formulation. Assuming harmonic solutions for eliminating the time

dependence, equations (A16) are rewritten in terms of x, y and θ as follows:

$$\left.\begin{aligned}
\frac{d^2}{dz^2}\left\{EI_{x1x1}\frac{d^2y}{dz^2} + EI_{x1y1}\frac{d^2x}{dz^2}\right\} &= \rho AP_n^2 y + \rho AP_n^2 r_x \theta \\
\frac{d^2}{dz^2}\left\{EI_{y1y1}\frac{d^2y}{dz^2} + EI_{x1y1}\frac{d^2x}{dz^2}\right\} &= \rho AP_n^2 x + \rho AP_n^2 r_y \theta \\
\frac{d}{dz}\left(C\frac{d\theta}{dz}\right) &= -\rho Ar_x P_n^2 y - \rho Ar_y P_n^2 x - \rho I_{cf} P_n^2 \theta
\end{aligned}\right\} \qquad \text{(A18)}$$

Equations (A18) agree with those derived earlier by Carnegie (ref. 10) for the specialized case considered here.

APPENDIX B

SHAPE FUNCTIONS, GEOMETRIC PROPERTIES, AND COEFFICIENTS OF DIFFERENTIAL EQUATIONS

Shape functions:

$$f_i(\eta) = \eta^i (R_1 \eta - R_2 \eta^2 + R_3 \eta^3)$$

$$g_i = R_4 (1-\eta)^i$$

$$h_i = \eta^i (1 - R_5 \eta)$$

$$G(t) = \sin Pt$$

$$H(t) = \cos Pt$$

$$R_1 = (i+2)(i+3)/6;\ R_2 = i(i+3)/3;\ R_3 = i(i+1)/6;\ R_4 = 1/(i+1);\ R_5 = i/(i+1)$$

Geometric properties:

$$r_x = r_{xo} \cos \gamma\eta - r_{yo} \sin \gamma\eta$$

$$r_y = r_{yo} \cos \gamma\eta - r_{xo} \sin \gamma\eta$$

$$I_{x1x1} = I_{yy} \sin^2 \gamma\eta + I_{xx} \cos^2 \gamma\eta$$

$$I_{y1y1} = I_{yy} \cos^2 \gamma\eta + I_{xx} \sin^2 \gamma\eta$$

$$I_{x1y1} = \left(\frac{I_{yy} - I_{xx}}{2} \right) \sin 2\gamma\eta$$

Coefficients of differential equations:

The coefficients of the differential equations given by equations (10 to 12) are given below.

$$a_1 = I_{yy} \sin^2 \gamma\eta + I_{xx} \cos^2 \gamma\eta$$

$$b_1 = 2\gamma \sin 2\gamma\eta\ (I_{yy} - I_{xx})$$

$$c_1 = 2\gamma^2 \cos 2\gamma\eta\ (I_{yy} - I_{xx})$$

$$d_1 = (I_{yy} - I_{xx}) \sin 2\gamma\eta/2$$

$$e_1 = 2\gamma \cos 2\gamma\eta\ (I_{yy} - I_{xx})$$

$$f_1 = -2\gamma^2 \sin 2\gamma\eta\ (I_{yy} - I_{xx})$$

$$a_2 = (I_{yy} - I_{xx}) \sin 2\gamma\eta/2$$

$$b_2 = 2\gamma \cos 2\gamma\eta\ (I_{yy} - I_{xx})$$

$$c_2 = -2\gamma^2 \sin 2\gamma n \, (I_{yy} - I_{xx})$$

$$d_2 = I_{yy} \cos^2 \gamma n + I_{xx} \sin^2 \gamma n$$

$$e_2 = -2\gamma \sin 2\gamma n \, (I_{yy} - I_{xx})$$

$$f_2 = -2\gamma^2 \cos 2\gamma n \, (I_{yy} - I_{xx})$$

$$g_1 = \rho A L^4 / E$$

$$h_1 = \rho A L^4 \, (r_{xo} \cos \gamma n - r_{yo} \sin \gamma n)/E$$

$$g_2 = g_1$$

$$h_2 = \rho A L^4 \, (r_{yo} \cos \gamma n + r_{xo} \sin \gamma n)/E$$

$$a_3 = 1; \; d_3 = \rho \, [I_{xx} + I_{yy} + A \, (r_{xo}^2 + r_{yo}^2)]/C$$

$$b_3 = \rho A \, (r_{xo} \cos \gamma n - r_{yo} \sin \gamma n)/C; \; n = i \, h$$

$$c_3 = \rho A \, (r_{yo} \cos \gamma n + r_{xo} \sin \gamma n)/C; \; h = L/n$$

REFERENCES

1. Duncan, W. J., Ellis, D. L., and Scruton, C.: The Flexural Center and the Center of Twist of an Elastic Cylinder. Philos. Mag., Series 7, vol. 16, no. 104, 1933, pp. 201-235.

2. Carnegie, William: Experimental Determination of the Center-of-Flexure and Center-of-Torsion Coordinates of an Asymmetrical Aerofoil Cross-Section. J. Mech. Eng. Sci. vol. 1, no. 3, 1959, pp. 241-249.

3. Subrahmanyam, K. B.; and Kaza, K. R. V.: Finite-Difference Analysis of Torsional Vibrations of Pretwisted, Rotating, Cantilever Beams with Effects of Warping. To be Published in J. Sound Vib., vol. 99, no. 1, 1985.

4. Wagner, H.: Torsion and Buckling of Open Section. NACA TM-807, 1936.

5. Garland, C. F.: The Normal Modes of Vibration of Beams having Noncollinear Elastic and Mass Axes. J. Appl. Mech., vol. 7, no. 3, Sept. 1940, pp. A97-105.

6. Gere, J. M.; and Lin, Y. K.: Coupled Vibrations of Thin-Walled Beams of Open Section. J. Appl. Mech., vol. 25, no. 3, Sept. 1958, pp. 373-378.

7. Houbolt, J. C.; and Brooks, W. G.: Differential Equations of Motion for Combined Flapwise Bending, Chordwise Bending and Torsion of Twisted Nonuniform Rotor Blades. NACA Rep. 1346, 1958.

8. Montoya, J.: Coupled Bending and Torsional Vibrations of a Twisted Rotating Blade. Brown Boveri Rev., vol. 53, no. 3, 1966, pp. 216-230.

9. Yu, Y. Y.: Variational Equation of Motion for Coupled Flexure and Torsion of Bars of Thin-walled Open Section Including Thermal Effect. J. Appl. Mech., vol. 38, June 1971, pp. 502-506.

10. Carnegie, W.: A Note One the Application of the Variational Method to Derive the Equations of Dynamic Motion of a Pretwisted Cantilever Blade Mounted on the Periphery of a Rotating Disc Allowing for Shear Deflection, Rotary Inertia and Torsion Bending. Bull. Mech. Eng. Educ., vol. 5, 1966, pp. 221-223.

11. Rao, D. K.; and Rao, J. S.: Equations of Motion of Rotating Pretwisted Blades in Bending-Bending-Torsion with Effects of Warping, Shear, Rotary Inertia etc. Proc. Silver Jubilee Cong. Aero. Soc. India. Paper No. 4.3, 1973.

12. Subrahmanyam, K. B.; Kulkarni, S. V.; and Rao, J. S.: Application of the Reissner Method to Derive the Coupled Bending-Torsion Equations of Dynamic Motion of Rotation Pretwisted Cantilever Blading with Allowance for Shear Deflection, Rotary Inertia, Warping and Thermal Effects. J. Sound Vib., vol. 84, no. 2, 1982, pp. 223-240.

13. Hodges, D. H.; and Dowell, E. H.: Nonlinear Equations of Motion for the Elastic Bending and Torsion of Twisted Nonuniform Rotor Blades. NASA TN-D-7818, 1974.

14. Rosen, A.; and Friedmann, P. P.: Nonlinear Equations of Equilibrium for Elastic Helicopter on Wind Turbine Blades Undergoing Moderate Deformation. UCLA-ENG-7718, University of California, Los Angeles, School of Engineering and Applied Science Report, 1978.

15. Kaza, K. R. V.; and Kvaternik, R. G.: Nonlinear Aeroelastic Equations for Combined Flapwise Bending, Chordwise Bending, Torsion and Extension of Twisted Non-Uniform Rotor Blades in Forward Flight. NASA TM-74059, 1977.

16. Rao, J. S.: Turbomachine Blade Vibration. Shock Vib. Dig., vol. 15, no. 5, 1983, pp. 3-9.

17. Leissa, Arthur: Vibrational Aspects of Rotating Turbomachinery Blades. Appl. Mech. Rev., vol. 34, no. 5, May 1981, pp. 629-635.

18. Greenwood, Donald T.: The Use of Higher Order Difference Methods in Beam Vibration Analysis. NASA TN-D-964, 1961.

19. Salvadori, M. G.: Numerical Computation of Buckling Loads by Finite Differences. Proc. Am. Soc. Civ. Eng. vol. 75, no. 10, Dec. 1949, pp. 1441-1475.

20. Subrahmanyam, K. B.; and Kaza, K. R. V.: An Improved Finite-Difference Analysis of Uncoupled Vibrations of Tapered Cantilever Beams. NASA TM-83495, Sept. 1983.

21. Subrahmanyam, K. B.; and Kaza, K. R. V.: An Improved Finite-Difference Vibration Analysis of Pretwisted, Tapered Beams. Proceedings, 12th Southeastern Conference on Theoretical and Applied Mechanics. vol. 1, Eng. Ext. Serv., Sch. Eng., Auburn Univ., 1984, pp. 118-126.

22. Reissner, E.: On a Variational Theorem in Elasticity, J. Math. Phys. vol. 29, 1950, pp. 90-95.

23. Subrahmanyam, K. B.; and Rao, J. S.: Coupled Bending-Bending Vibrations of Pretwisted Tapered Cantilever Beams Treated by the Reissner Method. J. Sound Vib., vol. 82, no. 4, 1982, pp. 577-592.

24. Dean, Thomas Scott; and Plass, H. J. Jr.: A Dynamic Variational Principle for elastic Bodies, and its Application to Approximations in Vibration Problems. Developments in Mechanics. Vol. 3, Part 2, T. C. Huang, and M. W. Johnson, Jr. eds., John Wiley and Sons, Inc., 1967, pp. 107-118.

25. Kumar, D.; Kulkarni, S. V.; and Subrahmanyam, K. B.: Uncoupled Vibrations of Tapered Cantilever Beams Treated by the Dean and Plass Dynamic Variational Principle. J. Sound Vib., vol. 79, no. 4, 1981, pp. 609-615.

26. Subrahmanyam, K. B.; Kulkarni, S. V.; and Rao, P. M.: Dean and Plass Method Calculations of Flexural Frequencies of Temoshenko Beams. J. Sound Vib., vol. 81, no. 1, Mar. 1982, pp. 141-146.

27. Leissa, A. W.; and Co, Chi-min: Coriolis Effects on the Vibrations of Rotating Beams and Plates. Proceedings, 12th Southeastern Conference on Theoretical and Applied Mechanics, vol. 2, Eng. Ext. Serv., Sch. Eng., Auburn Univ., 1984, pp. 508-513.

28. Dugundji, J.; and Wendell, J. H.: Some Analysis Methods for Rotating Systems with Periodic Coefficients. AIAA J., vol. 21, no. 6, 1983, pp. 890-897.

29. Carnegie, W.: Vibrations of Pretwisted Cantilever Blading. Proc. Inst. Mech. Eng., Vol. 173, No. 12, 1959, pp. 343-374.

30. Carnegie, W.; Dawson, B.; and Thomas, J.: Vibration Characteristics of Cantilever Blading. Proc. Inst. Mech. Eng., Vol. 180, pt. 3I, 1965-66, pp. 71-89.

31. Carnegie, W.; and Dawson, B.: Vibration Characteristics of Straight Blades of Asymmetrical Aerofoil Cross-Section. Aeronaut. Q., Vol. 20, 1968, pp. 178-190.

32. Rao, J. S.; and Carnegie, W.: Solution of the Equations of Motion of Coupled Bending-Bending-Torsion Vibrations of Turbine Blades by the Method of Ritz-Galerkin. Int. J. Mech. Sci., Vol. 12, 1970, pp. 875-882.

33. Dawson, B.; and Carnegie, W.: Modal Curves of Pretwisted Beams of Rectangular Cross-Section. J. Mech. Eng. Sci., Vol. 11, No. 1, 1969, pp. 1-13.

34. Richardson, L. F.: The Approximate Arithmetical Solution by Finite Differences of Physical Problems involving Differential Equations, with an Application to the Stresses in a Masonry Dam. Philos. Trans. R. Soc. London, Ser. A, vol. 210, no. IX, 1911, pp. 307-357.

35. Rosard, D. D.: Natural Frequencies of Twisted Cantilever Beams. J. Appl. Mech., vol. 20, no. 2, 1953, pp. 241-244.

36. The International Mathematical and Statistical Library (ISML), Houston, Texas, 1975.

TABLE I. - NUMERICAL DATA FOR AIRFOIL BLADES (ref. 30)

L	= 152.40 mm (6.0 in.)
A	= 589.68 sq mm (0.914 sq in.)
I_{xx}	= 34.963 mm^4 (0.000084 $in.^4$)
I_{yy}	= 2792.9 mm^4 (0.00671 $in.^4$)
E	= 213.73747 GPa (31×10^6 psi)
ρ	= 20.3444 kg/m^3 (0.284 $lbf/in.^3$)
r_{xo}	= 0.19304 mm (0.0076 in.)
r_{yo}	= 1.1938 mm (0.047 in.)

TABLE II. - TORSIONAL RIGIDITY OF PRETWISTED AIRFOIL BLADE (ref. 29)

Pretwist angle, γ, deg	Torsional rigidity, C	
	Nm^2/rad	$lb\ in.^2/rad$
0	9.1265	3180.1684
15	9.1759	3197.4
30	9.3269	3250.0
45	9.6282	3355.0
60	10.0440	3500.0
75	10.6470	3710.0
89	11.5600	4028.0

TABLE III. - CONVERGENCE PATTERN AND COMPARISON OF COUPLED BENDING-BENDING-TORSION FREQUENCIES: FIRST- AND SECOND ORDER FINITE-DIFFERENCE METHODS (Hz)

γ	Mode number	First order finite-difference method						Second order finite-difference method			
		n = 10	20	30	40	50	60	10	20	30	Extrapolated
0°	1	95.929	96.534	96.648	96.687	96.706	96.716	96.706	96.734	96.737	96.738
	2	581.449	599.808	603.358	604.613	605.196	605.513	603.475	605.911	606.141	606.204
	3	836.642	841.330	842.204	842.510	842.652	842.729	842.658	842.874	842.895	842.901
	4	1074.560	1076.166	1076.468	1076.574	1076.623	1076.650	1076.654	1076.704	1076.709	1076.710
	5	1557.277	1659.921	1680.532	1687.877	1691.301	1693.168	1672.018	1694.623	1696.647	1697.190
	6	2875.489	3087.379	3091.582	3093.051	3093.731	3094.100	3093.880	3094.862	3094.923	3094.937
	7	3064.882	3201.482	3269.552	3294.057	3305.523	3311.786	3207.516	3313.419	3322.705	3325.192
-30°	1	103.644	98.249	98.552	97.324	97.221	97.165	101.665	98.171	97.554	97.378
	2	384.472	482.100	501.378	508.273	511.493	513.251	464.308	507.565	513.490	515.149
	3	1032.234	988.711	980.034	976.911	975.446	974.645	1011.948	981.844	976.653	975.145
	4	1187.743	1109.888	1104.447	1102.855	1102.162	1101.796	1134.652	1105.379	1102.703	1101.983
	5	1187.743	1548.318	1607.632	1628.241	1637.768	1642.942	1490.641	1632.749	1647.241	1651.192
	6	2622.674	3089.437	3129.428	3133.785	3135.325	3136.082	3074.468	3139.478	3138.599	3138.141
	7	3112.428	3151.108	3213.081	3245.109	3260.536	3269.030	3136.994	3272.776	3286.343	3290.033

TABLE IV - COVERGENCE PATTERN OF COUPLED BENDING-BENDING-TORSION FREQUENCIES (Hz)

(a) Reissner method and Dean and Plass method using identical shape functions. $\gamma = 0^\circ$

Mode number	Number of terms in assumed solution, k					
	1	2	3	4	5	6
1	94.042	96.664	96.738	96.739	96.739	96.739
2	822.909	573.170	599.444	606.259	606.219	606.235
3	1079.098	842.363	842.903	842.904	842.904	842.904
4	--------	1076.708	1076.708	1076.711	1076.711	1076.711
5	--------	3183.905	1596.621	1629.061	1697.967	1696.414
6	--------	5216.526	3107.792	3095.274	3051.492	3094.935
7	--------	--------	5293.266	3210.000	3095.062	3328.162

(b) Reissner method and Dean and Plass method. $\gamma = -30^\circ$

Mode number	Number of terms in assumed solution, k					
	1	2	3	4	5	6
1	94.514	96.997	97.041	97.041	97.041	97.041
2	623.304	495.286	515.031	517.281	517.262	517.267
3	1072.483	960.023	962.517	972.845	972.777	972.809
4	--------	1097.665	1096.317	1100.997	1100.970	1100.990
5	--------	3180.700	1565.746	1600.834	1655.388	1653.893
6	--------	3693.199	3159.649	3066.255	3031.560	3137.568
7	--------	--------	5559.758	3187.625	3154.065	3291.277

TABLE V. - NATURAL FREQUENCIES OF DOUBLY SYMMETRIC PRETWISTED BLADES (Hz): SECOND ORDER FINITE-DIFFERENCE METHOD n = 30, $r_{xo} = r_{yo} = 0$

Mode number, classification	Uncoupled bending and torsion modes $r_{xo} = r_{yo} = \gamma = 0$	Coupled bending-bending modes and uncoupled torsion modes			
		$\gamma = 30^\circ$	$\gamma = 45^\circ$	$\gamma = 60^\circ$	$\gamma = 89^\circ$
1 (F1)	96.738	97.558	98.417	99.319	100.255
2 (F2)	606.158	513.908	454.448	403.476	330.908
3 (S1)	864.603	1014.142	1136.247	1250.120	1282.718
4 (T1)	1051.080	[a]1062.557	[a]1079.585	[a]1102.668	[a]1182.920
5 (F3)	1696.742	1648.125	1600.250	1562.417	1674.196
6 (T2)	3153.229	[a]3187.661	[a]3238.745	[a]3307.992	[a]3548.748
7 (F4)	3323.060	3281.225	3234.039	3176.773	3071.047
8 (T3)	5255.263	[a]5312.648	[a]5397.786	[a]5513.196	[a]5914.446
9 (S2)	5417.605	5242.015	5149.207	5047.868	4815.582
10 (F5)	5488.150	5815.830	6086.129	6417.764	7315.336

[a]Uncoupled torsional frequency of pretwisted blade.

TABLE VI. - COUPLED FREQUENCIES (Hz.) OF PRETWISTED BLADES WITH ASYMMETRY ABOUT ONE PLANE: $r_{xo} = 0.193$ mm, $r_{yo} = 0$

Mode number	Uncoupled frequency $r_{xo} = r_{yo} = \gamma = 0$	Coupled bending-torsion frequency, $\gamma = 0$	Coupled bending-bending-torsion frequency			
			$\gamma = 30^\circ$	$\gamma = 45^\circ$	$\gamma = 60^\circ$	$\gamma = 89^\circ$
1	96.738 (F1)	96.737	97.558	98.417	99.319	100.255
2	606.158 (F2)	606.142	513.891	454.432	403.461	330.898
3	864.603 (S1)	[a]864.603	1013.977	1136.514	1250.296	1283.036
4	1051.080 (T1)	1051.095	1062.743	1079.348	1102.544	1182.623
5	1696.742 (F3)	1696.647	1648.040	1600.157	1562.299	1674.142
6	3153.229 (T2)	3153.270	3187.303	3245.592	3309.104	3549.324
7	3323.060 (F4)	3322.728	3281.327	3226.973	3175.471	3070.251

[a]Uncoupled flexural mode in chordwise direction.

TABLE VII. - COUPLED FREQUENCIES (Hz) OF PRETWISTED BLADES WITH ASYMMETRY ABOUT ONE PLANE: $r_{xo} = 0$, $r_{yo} = 1.1938$ mm

Mode number	Uncoupled frequency $r_{xo} = r_{yo} = \gamma = 0$	Coupled bending-torsion frequency, $\gamma = 0$	Coupled bending-bending-torsion frequency			
			$\gamma = 30^\circ$	$\gamma = 45^\circ$	$\gamma = 60^\circ$	$\gamma = 89^\circ$
1	96.738 (F1)	[a]96.738	97.556	98.412	99.311	100.246
2	606.158 (F2)	[a]606.158	513.342	454.127	403.354	330.907
3	864.603 (S1)	842.893	974.417	1170.423	1264.208	1289.706
4	1051.080 (T1)	1076.696	1105.563	1047.110	1088.446	1174.069
5	1696.742 (F3)	[a]1696.742	1647.418	1599.494	1561.908	1671.711
6	3153.229 (T2)	3094.865	3131.506	3270.061	3304.629	3542.868
7	3323.060 (F4)	[a]3323.060	3290.388	3166.320	3154.937	3069.589

[a]Uncoupled flexural mode in flapwise direction.

TABLE VIII. - COUPLED BENDING-BENDING-TORSION FREQUENCIES OF ASYMMETRIC AIRFOIL BLADE (Hz): $r_{xo} = 0.193$ mm, $r_{yo} = 1.1938$ mm

Mode number	Uncoupled frequency $r_{xo} = r_{yo} = \gamma = 0$	Coupled bending-bending-torsion frequency				
		$\gamma = 0$	$\gamma = 30^\circ$	$\gamma = 45^\circ$	$\gamma = 60^\circ$	$\gamma = 89^\circ$
1	96.738 (F1)	96.737	97.557	98.413	99.313	100.246
2	606.158 (F2)	606.141	513.162	453.978	403.259	330.896
3	864.603 (S1)	842.895	972.178	1174.357	1267.441	1292.688
4	1051.080 (T1)	1076.709	1108.465	1043.971	1085.937	1170.910
5	1696.742 (F3)	1696.647	1647.424	1599.445	1562.017	1672.784
6	3153.229 (T2)	3094.922	3124.353	3277.243	3308.751	3539.662
7	3323.060 (F4)	3322.705	3294.018	3154.608	3145.672	3067.755

TABLE IX. - COMPARISON OF CPU TIMES (milliseconds) REQUIRED BY DIFFERENT METHODS FOR PRETWISTED AIRFOIL BLADE CASE USING EIGZF ROUTINE: $\gamma = -30^{\circ}$, $r_{xo} = 0.193$ mm, $r_{yo} = 1.1938$ mm

Number of beam segments n	Finite-difference method		Number of terms in assumed solutions K	Mixed variational principle	
	I order	II order		Reissner	Dean and Plass
10	831	856	1	59	84
20	5 550	5390	2	215	348
30	17 736	17014	3	490	847
40	41 484	-----	4	924	1639
50	76 966	-----	5	1494	2881
60	225 838	-----	6	2193	4410

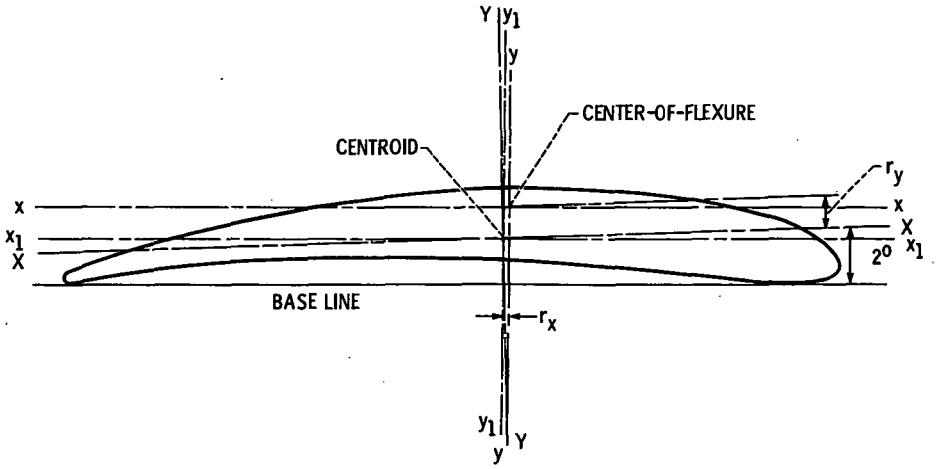

Figure 1. - Cross-section of asymmetrical airfoil blade showing position of the centroid and center-of-flexure.

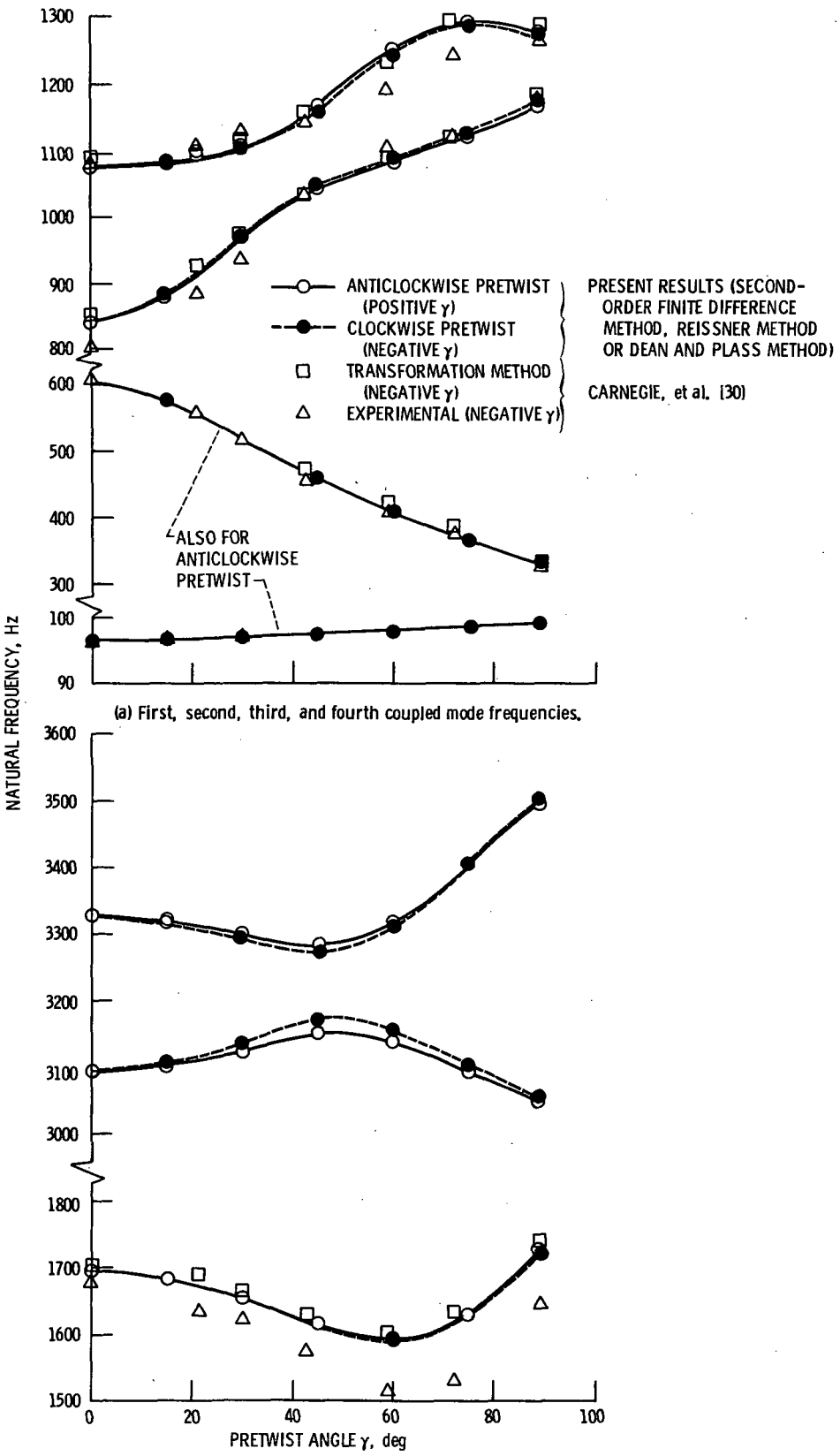

(a) First, second, third, and fourth coupled mode frequencies.

(b) Fifth, sixth, and seventh coupled mode frequencies.

Figure 2. - Comparison of theoretical and experimental coupled bending-bending-torsion frequencies.

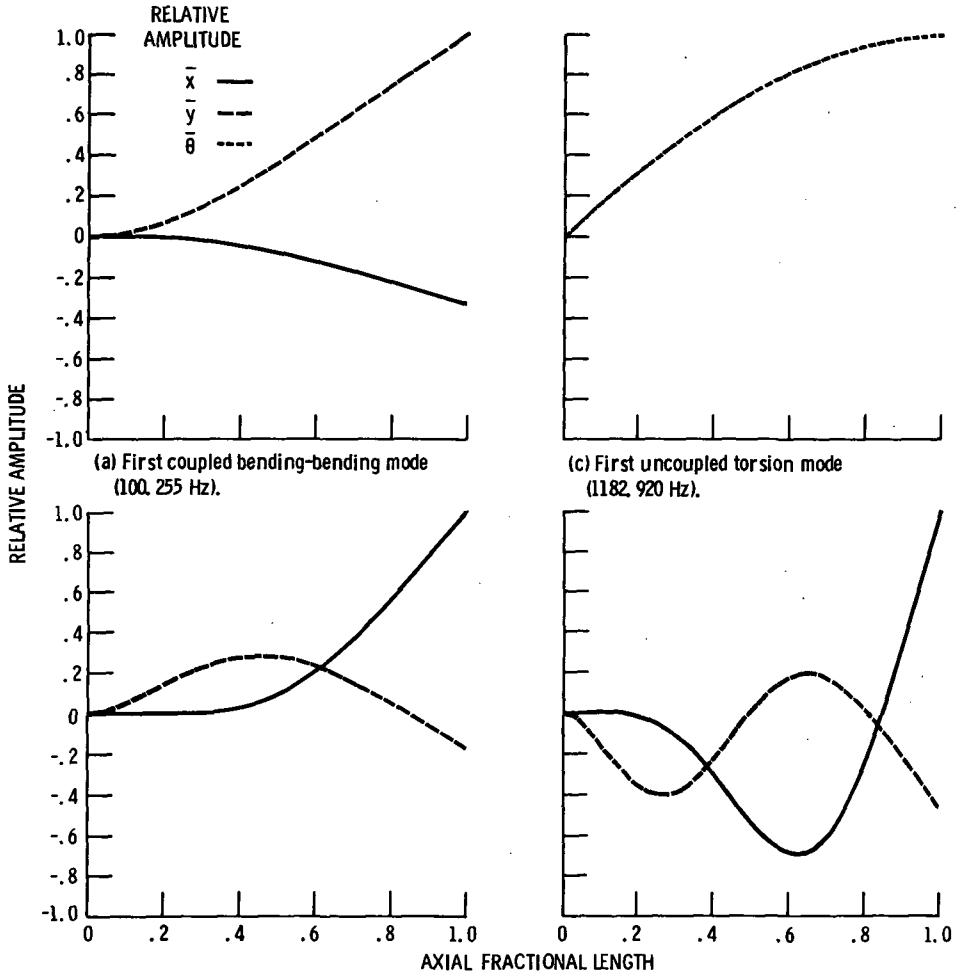

(a) First coupled bending-bending mode (100.255 Hz).

(c) First uncoupled torsion mode (1182.920 Hz).

(b) Second coupled bending-bending mode (330.908 Hz).

(d) Third coupled bending-bending mode (1282.718 Hz).

Figure 3. - Coupled bending-bending, and uncoupled torsion mode shapes of a pretwisted blade of doubly symmetric cross section. $r_{xo} = r_{yo} = 0$, $\gamma = 89^{o}$.

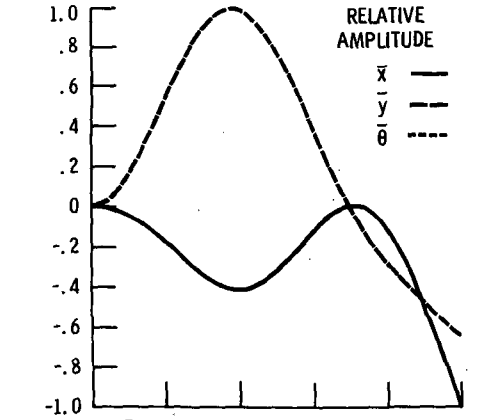

(e) Fourth coupled bending-bending mode (1674.196 Hz).

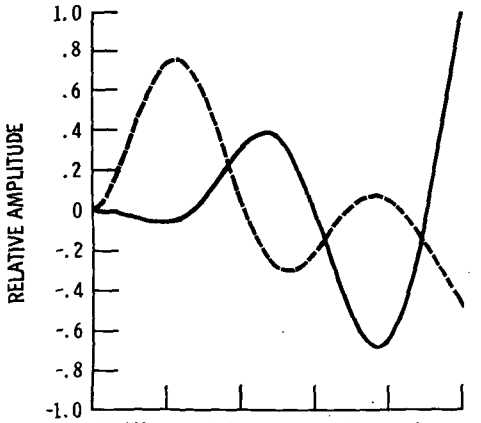

(f) Fifth coupled bending-bending mode (3071.047 Hz).

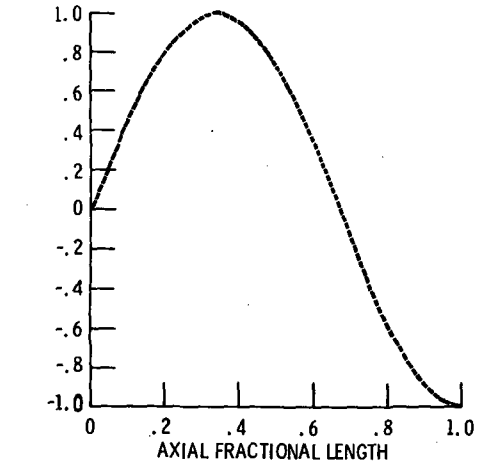

(g) Second uncoupled torsion mode (3548.748 Hz).

Figure 3. - Concluded.

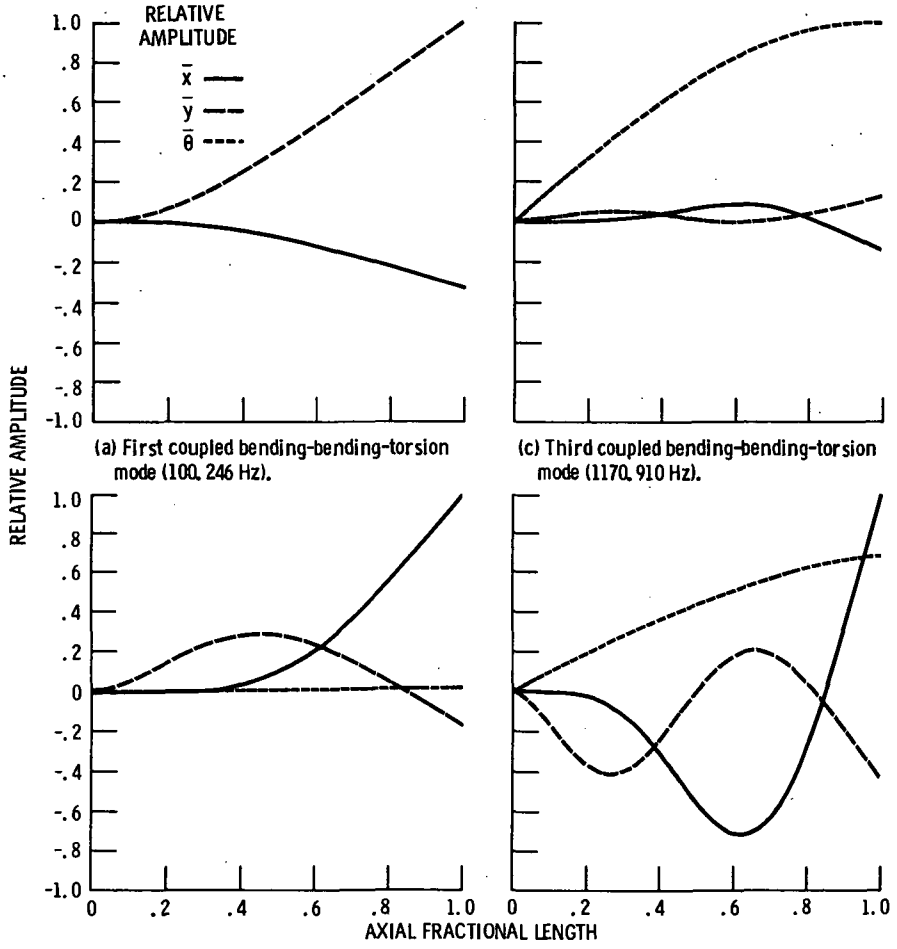

(a) First coupled bending-bending-torsion mode (100.246 Hz).

(c) Third coupled bending-bending-torsion mode (1170.910 Hz).

(b) Second coupled bending-bending-torsion mode (330.896 Hz).

(d) Fourth coupled bending-bending-torsion mode (1292.688 Hz).

Figure 4. - Coupled bending-bending-torsion mode shapes of a pretwisted asymmetric airfoil blade. r_{xo} = 0.19304 mm (0.0076 in), r_{yo} = 1.1938 mm (0.047 in), $\gamma = 89^{0}$.

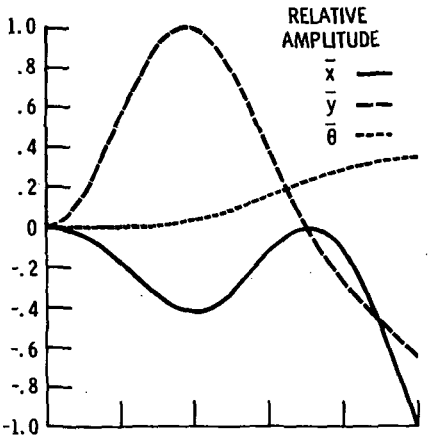

(e) Fifth coupled bending-bending-torsion mode (1672.784 Hz).

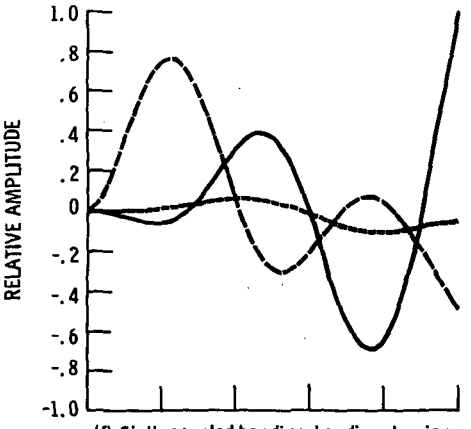

(f) Sixth coupled bending-bending-torsion mode (3067.755 Hz).

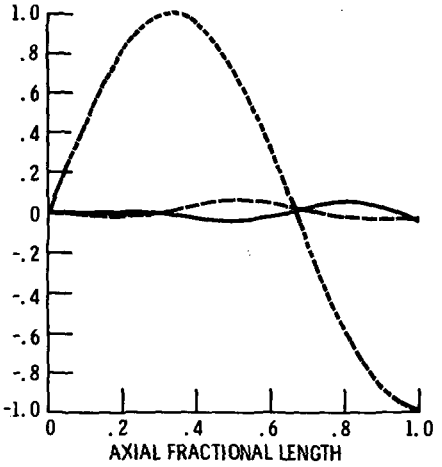

(g) Seventh coupled bending-bending-torsion mode (3539.662 Hz).

Figure 4. - Concluded.

1. Report No.	2. Government Accession No.	3. Recipient's Catalog No.
NASA TM-83735		

4. Title and Subtitle	5. Report Date
Improved Methods of Vibration Analysis of Pretwisted, Airfoil Blades	6. Performing Organization Code: 505-33-42

7. Author(s)	8. Performing Organization Report No.
K. B. Subrahmanyam and K. R. V. Kaza	E-2175
	10. Work Unit No.

9. Performing Organization Name and Address	11. Contract or Grant No.
National Aeronautics and Space Administration Lewis Research Center Cleveland, Ohio 44135	13. Type of Report and Period Covered: Technical Memorandum

12. Sponsoring Agency Name and Address	14. Sponsoring Agency Code
National Aeronautics and Space Administration Washington, D.C. 20546	

15. Supplementary Notes

K. B. Subrahmanyam, NBKR Institute of Science and Technology, Mechanical Engineering Dept., Vidyanagar 524 413, India and NRC-NASA Research Associate; K. R. V. Kaza, Lewis Research Center. Prepared for the XVIth International Congress of Theoretical and Applied Mechanics cosponsored by the International Union of Theoretical and Applied Mechanics (IUTAM) and the Technical University of Denmark, Lyngby, Denmark, August 19-25, 1984.

16. Abstract

Vibration analysis of pretwisted blades of asymmetric airfoil cross section is performed by using two mixed variational approaches, one proposed by Dean and Plass, and the other by Reissner. Numerical results obtained from these two methods are compared to those obtained from an improved finite-difference method developed by the authors, and also to those given by the ordinary finite-difference method. The relative merits, convergence properties and accuracies of all four methods are studied and discussed. The effects of asymmetry and pretwist on natural frequencies and mode shapes are investigated. The improved finite-difference method is shown to be far superior to the conventional finite-difference method in several respects. Close lower bound solutions are provided by the improved finite-difference method for untwisted blades with a relatively coarse mesh while the mixed methods have not indicated any specific bound.

17. Key Words (Suggested by Author(s))	18. Distribution Statement:
Blade vibration Reissner method Dean and Plass method Finite-difference methods	Unclassified - unlimited STAR Category 39

19. Security Classif. (of this report)	20. Security Classif. (of this page)	21. No. of pages	22. Price*
Unclassified	Unclassified		

*For sale by the National Technical Information Service, Springfield, Virginia 22161

National Aeronautics and
Space Administration

Washington, D.C.
20546

Official Business
Penalty for Private Use, $300

SPECIAL FOURTH CLASS MAIL
BOOK

Postage and Fees Paid
National Aeronautics and
Space Administration
NASA-451

NASA

POSTMASTER: If Undeliverable (Section 158
Postal Manual) Do Not Return